HIGHER-ABSTRACTION LOCAL BINARY PATTERN: A NOVEL DESCRIPTOR FOR IMAGE RETRIEVAL

M.Tech. Thesis

By

SAURABH SONI

(Roll No. MT1502102009)

DISCIPLINE OF ELECTRICAL ENGINEERING

INDIAN INSTITUTE OF TECHNOLOGY INDORE

JUNE 2017

HIGHER-ABSTRACTION LOCAL BINARY PATTERN: A NOVEL DESCRIPTOR FOR IMAGE RETRIEVAL

A THESIS

Submitted in partial fulfillment of the requirements for the award of the degree

of

Master of Technology

with specialization in

Communication and Signal Processing

by

SAURAB H SONI

(Roll No. MT1502102009)

DISCIPLINE OF ELECTRICAL ENGINEERING

INDIAN INSTITUTE OF TECHNOLOGY INDORE

JUNE 2017

INDIAN INSTITUTE OF TECHNOLOGY INDORE

CANDIDATE'S DECLARATION

I hereby certify that the work which is being presented in the thesis entitled "**Higher-Abstraction local binary pattern, a novel descriptor for image retrieval**" in the partial fulfillment of the requirements for the award of the degree of **MASTER OF TECHNOLOGY** with specialization in **COMMUNICATION AND SIGNAL PROCESSING** and submitted in the **DISCIPLINE OF ELECTRICAL ENGINEERING, Indian Institute of Technology Indore**, is an authentic record of my own work carried out during the time period from JULY 2016 to JUNE 2017 under the supervision of Dr. Vivek Kanhangad, Associate Professor, Discipline of Electrical Engineering.

The matter presented in this thesis has not been submitted by me for the award of any other degree of this or any other institute.

Signature of the student with date
SAURABH SONI

This is to certify that the above statement made by the candidate is correct to the best of my knowledge.

Signature of the Thesis Supervisor
DR. VIVEK KANHANGAD

SAURABH SONI has successfully given his M.Tech. Oral Examination held on **1st July 2017**.

Signature of Supervisor of M.Tech. Thesis
Date:

Convener, DPGC
Date:

Signature of PSPC Member #1
Date:

Signature of PSPC Member #2
Date:

ACKNOWLEDGEMENTS

At first I would like to express my sincere gratitude to my supervisor, Dr. Vivek Kanhangad for his encouragement, support and guidance during my post-graduation and thesis work. He has always been my source of inspiration during my stay at IIT Indore and shall be, all my life.

I am thankful to all the faculty members for teaching me during my course work, which laid a strong foundation which eventually has helped me a lot to pursue further research.

It is my greatest pleasure to have Dr. Srivathsan Vasudevan and Dr. Shanmugam Dinakaran as my thesis committee members. They enhanced the level of my work by their thoughtful questioning and comments. I express my profound gratitude for them.

I am thankful to my senior Mr. Ashwani Kumar Tiwari for helping me in solving queries with his satisfactory solutions. He has been an inspirational person for me throughout my research work.

My sincere thanks to IIT Indore's all research lab mates who have helped me directly or indirectly for my project work, for all their unintentional and unconditional support. The entire journey of master's program was delighted with their presence.

I am inspired by my internship manager at Intel Corporation Bangalore, Mr. Ayan Roy Chowdhury. His immense passion for work made me enthusiastic and hardworking person. I am thankful to him for all his support.

My colleagues Ashish, Neetu, Anish, Khushbu, Anuj, Parual, Sushree, Ashima, Sarthak and all other friends have been supportive throughout my post-graduation. They made my life relaxed and hopeful. I am blessed to have friends like them. My hearty thanks for them.

Saurabh Soni,

M.Tech. (Communication and Signal Processing).

Mt1502102009.

Discipline of Electrical Engineering.

Indian Institute of Technology Indore (M.P.).

Dedicated to my parents

ABSTRACT

Local binary pattern (LBP) is the most commonly used feature descriptor. Many of the LBP variants are widely used in content-based image retrieval (CBIR) system because of their superior discrimination property.

Retrieving an image with high precision and recall rate is a challenge. The reason being, the dynamic texture properties and large number of images in the database. The color, shape, and texture information or combination of these attributes is known as the feature of an image which is used for image retrieval in the CBIR system. LBP utilizes texture information of neighboring pixels as feature which helps in the texture classification of images. Many of the available descriptors use LBP for multiple applications such as classification, shape localization, retrieval and face recognition. If an n-bit pattern has m-state changes of bits then, to define a uniform pattern m must be less than or equal to two. If m is greater than two then, it will represent non-uniform patterns.

The uniform pattern; an important property of image texture, together with LBP is used to obtain robust texture features for gray scale and multiresolution rotation invariant classification. It is hard to meet the requirement of "high precision and recall rate" for image retrieval. LBP has less computational complexity and better discrimination ability, but it is not possible to perform high abstraction of all the relevant features at center pixel. The term higher abstraction signifies the amount of information of surrounding neighborhood pixels for a particular center pixel.

The major concern of LBP is to obtain more information of local neighborhood at center pixel with better recall and precision rate for large database of images in CBIR system. Many texture descriptors have been proposed for improving the accuracy of retrieval system, but the issue of higher abstraction is considered in HA-LBP. In LBP, a single local descriptor for a specified center pixel is used, whereas in HA-LBP, multiple nearby descriptors are employed for a given center pixel to generate higher abstraction of neighborhood pixels. HA-LBP is generic in the sense that the same coding scheme can be utilized to code the binary output image as obtained from various descriptors viz. LDP, LTP, etc. The proposed HA-LBP is efficient in retrieval of images in CBIR system. We performed experiments on three benchmark publicly available image databases i.e. COREL-1K, GHIM-10K, and Brodatz texture database. The experiments resulted in significant improvement of 5.6%, 7.47% and 2.36% in average precision

rate and 3.65%, 2.81% and 2.36% in average recall rate for COREL-1K and GHIM-10K, and Brodatz databases respectively.

TABLE OF CONTENTS

Chapter 4: Proposed descriptor: Higher-Abstraction LBP (HA-LBP)

Chapter 5: Experimental results and comparison

Chapter 6: Conclusion and scope for future work

LIST OF FIGURES

LIST OF TABLES

LIST OF ABBREVIATIONS

CBIR	Content-based image retrieval.
LBP	Local binary patters.
LDP	Local derivative patterns.
LTP	Local ternary patterns.
LTrP	Local tetra patterns.
LMEBP	Local maximum edge binary patterns.
LGBP	Local Gabor binary patterns.
LTriDP	Local tri-directional patterns.
NRLBP	Noise resistant local binary patterns.
RLTP	Relaxed local ternary patterns.
LBP-HF	Histogram Fourier local binary patterns.
EEG	Electroencephalogram.
SVM	Support vector machine.
HALBP	High abstraction local binary patterns.
L1-HALBP	Level-1 high abstraction local binary patterns.
L2-HALBP	Level-2 high abstraction local binary patterns.

Chapter 1

Introduction

1.1 Literature review

CBIR system has an enormous literature due to its highly demanding applications in modern science and advanced technologies [1]. CBIR system has been successfully employed in medical imaging field [2]. Many feature descriptors have been constructed and several algorithms have been proposed to improve performance of image retrieval system. In this succession of advancements in the retrieval system, Ojala *et al*. [3] proposed the idea of LBP. It is a pixel intensity dependent texture descriptor. At first, the difference of gray values of all the neighbor pixels with respect to gray value of center pixel is obtained and the differences are quantized to either 0 or 1 to have a binary code. Finally, the decimal weight of obtained binary code is considered as LBP feature for a particularly given center pixel.

For a binary bitwise pattern, if state transitions of bits are less than or equal to two, then it is defined as the uniform pattern. Uniform patterns are the essential property of LBP, this work of LBP has been extended for multi-resolution and rotation invariant classification of texture [4, 5]. Together with LBP, the uniform measure of patterns is a local image texture configuration. The contrast of local image texture has been characterized by rotation invariant variance measures. The joint distribution of these orthogonal measures is computed which results in an excellent tool for analysis of rotation invariant texture.

A completed LBP proposed by Guo *et al*. [6] considered both sign and the magnitude of differences between center pixel and neighbor pixels. There exist many variants of the LBP in the literature such as the joint LBP with Gaussian mixtures and joint distribution [7], LBP variance with global matching [8], dominant LBPs [9], retrieval of images for biomedical applications [10], wavelet packets were used for feature extraction and together with Gabor filter applied for image retrieval [11].

Zhang *et al.* [12], proposed local derivative pattern (LDP) as dealt with four different (i.e. 0º, 45º, 90º and 135º) directional derivatives. LDP is encoded by concatenating the various directional derivatives which are computed by comparing the differences between the center pixel and its neighborhood pixels in each direction separately. It is further extended to n^{th} order LDP which is used in face recognition. Local ternary pattern (LTP) [13] has been encoded by using three levels (-1, 0, 1) of quantization for assigning ternary code to differences between gray value of center pixel and gray values of neighbor pixels. LTP outperformed in different lightening conditions where the impact of noise is dominant. Murala *et al*. [14], introduced local tetra patterns (LTrP) for CBIR, which are obtained by considering horizontal and vertical derivatives (0ºand 90º) of LDP [20] to get directionality for each pixel. Higher order derivative effectively utilized for face identification in local vector patterns [15]. In local Gabor binary patterns (LGBP) [16], LBP operator is applied on Gabor magnitude map which is generated by breaking up the input image considering a set of multi-scale and multi-orientation feature based on Gabor filters. Verma *et al*. [17] appended two more directions *i.e*. previous pixel direction and next pixel direction with the direction of center pixel as stated in LBP [3] to obtain local tri-directional pattern (LTrDP). Authors in [17] made use of directional patterns and magnitude pattern to encode LTrDP. For content-based image retrieval, extremes in particular direction are employed in the directional extreme patterns [18].

The local maximum edge binary pattern (LMEBP) [19] obtained the information based on local differences between neighborhood pixels and center pixel. LMEBP with the Gabor transform has been successfully utilized in image retrieval. The LBP histogram Fourier (LBP-HF) features [20], that is rotation invariant, generated considering cyclic shift property of discrete Fourier transform. Noise resistant LBP (NRLBP) proposed by Ren *et al.* [21], reduced the sensitivity to noise in pixel differences. The performance of image retrieval system under noisy conditions has been improved by relaxed local ternary pattern (RLTP) [22]. LBP is successfully used as key points for automated epilepsy diagnosis [23]. Recently a new revolutionary approach of histogram refinement using local skew pattern and binary eigenvalue map has been proposed [24]. Apart from given review of LBP, there are many applications of computer vision and image processing where LBP has been successfully applied for CBIR [25], object and face identification [26], facial appearances analysis [27-29], and shape localization [30]. Moreover, there exist several extensions of LBP in the past reported works [31-41].

1.2 Motivation

The meteoric advancements in CBIR help in retrieving a query image from the large database. It is a more encouraging task for a researcher to propose new algorithms to retrieve images with high precision rate and recall rate as the size of databases is increasing rapidly. The texture, color, shape, or rotation information or a combination of this information of an image represents the feature that is used to match query image with given image database in CBIR system. In [1], authors have described literature of texture descriptor in image retrieval and in [2] specified the application of CBIR in the field of medical imaging.

LBP [3] has arisen as precious texture descriptor in the era of texture analysis. In [24], the performance of existing texture descriptors has been improved by new methodology of histogram refinement. In such a large enhancement of texture based image analysis still, there is a lack of strong texture descriptor that can provide a confined abstraction of information of neighborhood pixels for a particular center pixel to precisely acquire a correct image for a query image from the massive database of images in the matching of feature vectors. This challenge has inspired us to design an algorithm that satisfactorily meets the requirement of higher abstraction of information from the neighborhood of corresponding pixels of the image for CBIR system.

1.3 Summary of contribution

In the proposed work, our primary objective is to create a local descriptor which has a higher abstraction of its neighborhood. To achieve our goal, we developed a coding scheme that considers multiple local patterns to obtain code for a particular center pixel.

However, the challenges were not completed yet, apart from this new concept the computational complexity has been increased due to consideration of multiple nearby local descriptors for pattern generation. We have reduced the redundancy by dividing the pattern into four directional classes according to nearby neighborhood pixels i.e. class-45, class-90, class-135, and class-180, for 45^0, 90^0, 135^0, and 180^0 respectively. Memory constraint was the major issue in performing the experiment on huge dataset such as GHIM 10K, which has been solved by redundancy reduction technique.

The performance of proposed HA-LBP has further improved by the reduced uniform pattern which is intended sub-type of the uniform patterns. A uniform pattern employs circular peripheral and allows maximum two transitions of states of bits and reduced uniform pattern encloses all ones in its periphery, which is minimum bounding rectangular.

The implementation of proposed method with accurate computation and analysis of results comparison with existing methods were the main work that has been contributed.

1.4 Thesis organization

The further structure of the thesis is as follows:

- In Chapter 2, LBP generation methodology discussed in detail in section 2.2 and some applications of LBP have been described in section 2.3.

- In Chapter 3, a brief description of some of the existing image retrieval methods has been portrayed. In Section 3.2, 3.3, and 3.4, local derivative patterns (LDP), local ternary pattern (LTP), and local tetra pattern (LTrP), explained respectively.

- In Chapter 4, the proposed (HA-LBP) texture descriptor methodology has been discussed.

- In Chapter 5 describes databases used for performance evaluation, followed by experimental results and discussion.

- In Chapter 6, the conclusions are drawn, and scope for future work has been discussed.

Chapter 2

Local binary patterns: an overview

2.1 Overview

In this chapter, the encoding algorithm of LBP and its significance is explained in detail. Uniform local binary patterns are described in section 2.3.

2.2 Formulation of LBP

LBP was proposed by Ojala *et al.* [3]. The LBP for a center pixel computed as considering differences between neighborhood pixels and center pixel and thresholding these differences using two level quantization (1 for positive values and 0 for negative values), as seen in Fig. 2.1, based on,

$$LBP_{N,r} = \sum_{n=1}^{N} (2^n - 1) \times B(P_n - P_c) \tag{1}$$

$$B(z) = \begin{cases} 1, & if \;\; z \geq 0 \\ 0, & else \end{cases} \tag{2}$$

Where N is number of neighborhood pixels, r is radius to represent periphery of the neighbors, P_n is gray value of n^{th} neighbor pixel, P_c is gray value of the center pixel.

A 3×3 matrix representation of gray values of sample image is shown in Fig. 2.1 (a-b). To encode the LBP at first, the differences of neighborhood pixels with respect to center pixel have been calculated and then, a threshold is applied according to Eq. (2) which elaborates that if the difference is greater than or equal to 0, the binary value 1 is assigned else binary value 0 is assigned. According to Eq. (1), a decimal weight with respect to pixel position is multiplied to obtained binary bit values and they are added to compute the LBP as shown in Fig. 2.1 (c-e).

G_1	G_2	G_3
G_8	$\boldsymbol{G_C}$	G_4
G_7	G_6	G_5

(a)

6	9	15
25	**11**	13
33	5	2

(b)

0	0	1
1	$\boldsymbol{G_C}$	1
1	0	0

(c)

1	2	4
128	$\boldsymbol{G_C}$	8
64	32	16

(d)

0	0	4
128	**204**	8
64	0	0

(e)

Figure 2.1. (a) A sample 3×3 pixel matrix with center pixel G_C. (b) An example 3×3 pixel gray value representation. (c) The binary representation of neighborhood pixels on center pixel. (d) 8-bit decimal weight matrix. (e) Obtained LBP by multiplying bit pattern (c) to their corresponding decimal weights (d).

2.3 Uniform local binary patterns

Let consider the radius r of circular LBP to be 1 therefore, there are eight neighboring pixels of a particularly given center pixel. If the binary pattern employs maximum two states shift of bits from 1 to 0 or vice versa, then it is called uniform pattern [16].

As shown in Table 2.1, the patterns 00000000 (0 state change), 00011000 (2 state changes) and 11000001 (2 state changes) are uniform and the patterns 00110110 (4 state changes) and 11010101 (6 state changes) are non-uniform patterns.

Table 2.1: Pattern bifurcation based on state changes of bits

8-bit circular pattern	Number of state changes (from 1 to 0 Or 0 to 1)	Type of pattern
00000000	0	Uniform
00011000	2	Uniform
11000001	2	Uniform
00110110	4	Non-uniform
10110001	4	Non-uniform
11010101	6	Non-uniform

To map a LBP to uniform LBP, there are separate classes of different sub-patterns which are uniform and one single class of non-uniform pattern. There are $n(n-1)+3$ classes (including non-uniform patterns) for n bit of uniform patterns [16]. Hence, 8-bit of uniform pattern consists of 59 classes, in which 58 classes have separate sub-patterns and remaining one class consists non-uniform patterns.

Ojala *et al*. [3] in their analysis, concluded that 90% of the patterns are uniform in radius-1 neighborhood (8, 1), and 70% of the patterns are uniform in radius-2 neighborhood (16, 1), thus uniform patterns are considered over non-uniform patterns.

2.4 Significance of local binary patterns

LBP has revolutionary impact on CBIR system and various classification, recognition and localization operations. LBP [3] has been applied to rotation invariant and gray scale texture classification together with uniform patterns and sample distribution of nonparametric discrimination. Uniformity in patterns grants a vast majority of local texture microstructures like edges of the image. Statistical and structural texture analysis can be done through this local texture patterns.

In the past years, LBP has been used in many applications of computer vision and image analysis, such as for texture classification [3-5], CBIR system [14, 25], recognition applications [16, 26], facial analysis [27-29], and localization of shape [30]. In the Biomedical domain, LBP emerged as a significant descriptor. If there is an excessive and sudden electrical discharge in cells of the human brain, it is called seizure which is the leading cause for neurological disorder named as epilepsy. Electroencephalogram signals (EEG) are primarily used for diagnosis of neurological disorders such as epileptic seizures [31, 32]. Approximately world's 1% of the population is affected by the Epilepsy [33-35], this neurological disorder is a vast area of interest for researchers now-a-days. Automated diagnosis of epilepsy has been provided by key point LBP of EEG signal [23]. In this method, arrangements of key points in EEG signals at multiple scales are done using a pyramid of the filtered signals, which is generated through difference of Gaussian filter. A feature set is created considering computed LBP at this key points, which is utilized in classification of EEG signals through SVM classifier.

Chapter 3

Traditional Local Patterns

3.1 Overview

In this chapter, LDP, LTP and LTrP have been explained. Mathematical computation of each descriptor has been described with the help of pictorial representation.

3.2 Local derivative patterns (LDP)

Zhang *et al.* [12], introduced LDP which is used for face recognition application. LDP grabs higher-order information at the center pixel by encoding different spatial relationships with the local neighborhood. Gabor feature images and gray value images are used to evaluate the performance of LDP and LBP. LDP encodes comparisons between derivative directions at center pixel and its neighbor pixels. It interrogates effectiveness and feasibility of higher-order patterns for the face recognition.

The LDP operator compute binary coded function which is based on directional variations of higher order derivatives. LBP uses first order derivative in all directions to get a binary code while, all the higher order derivatives in four directions (i.e. 0^0, 45^0, 90^0, and 135^0) have been used in LDP to encode binary function which consists of more discriminative information of texture feature that cannot be captured by first order LBP.

Let assume radius-1 3×3 sample matrix having eight neighborhoods (G_1, G_2, G_3, G_4, G_5, G_6, G_7, and G_8) for a given center pixel G_c as shown in Fig. 3.1 (a). LDP for given directions 0^0, 45^0, 90^0, and 135^0, obtained corresponding to G_4, G_3, G_2 and G_1 with respect to G_c respectively. LDP in all four stated directions have been computed by using Eq. (3) to (10). The function $p(a,b)$ from Eq. (3) has been applied to encode gray value differences into feature.

$$p(G_C, G_i) = \begin{cases} 0, & if\ G(i) - G(c) \leq Threshold\ ; \\ 1, & if\ G(i) - G(c) > Threshold; \end{cases} \quad Where\ i = 1,2,3, \ldots 8; \tag{3}$$

$$G_{LDP}^{0}(C) = G(c) - G(4)\ ; \tag{4}$$

$$G_{LDP}^{45}(C) = G(c) - G(3)\ ; \tag{5}$$

$$G_{LDP}^{90}(C) = G(c) - G(2)\ ; \tag{6}$$

$$G_{LDP}^{135}(C) = G(c) - G(1)\ ; \tag{7}$$

$$LDP_{\theta}^{2}(G_C) = \{P(G'_C, G'_1), P(G'_C, G'_2), P(G'_C, G'_3) \ldots \ldots \ldots . . P(G'_C, G'_8)\ \} \tag{8}$$

$$P(G'_C, G'_i) = \begin{cases} 0, & if\ G'_C . G'_i > 0; \\ 1, & if\ G'_C . G'_i \leq 0; \end{cases} where\ i = 1,2,3, \ldots \ldots 8 \tag{9}$$

$$LDP^{2}(G_C) = \{LDP_{\theta}^{2}(G_C)\} \big| \theta = 0^0, 45^0, 90^0, 135^0; \tag{10}$$

G_1	G_2	G_3
G_8	$\boldsymbol{G_C}$	G_4
G_7	G_6	G_5

(a)

2	1	5	6	4
3	7	2	1	9
5	5	**3**	7	6
6	4	5	4	3
1	3	9	7	1

(b)

Figure 3.1. (a) A sample 3×3 matrix with center pixel G_c . (b) An example 5×5 matrix of an image having 3 as center pixel.

The four possible structures of four directions have been shown in Fig. 3.2 and Table 3.1 illustrate these combinations. Binary code of all possible combinations required for computation of LDP is generated using Eq. (3) as per structures given in Fig. 3.2. In Table 3.1, it is elaborated that, the structure $S_{LDP}(1)$ for four angles i.e. 0^0, 45^0, 90^0, and 135^0 use function $p(G_c, G_1)$ and $p(G_c, G_5)$ from Eq. (3). Similarly, $S_{LDP}(2)$, $S_{LDP}(3)$, and $S_{LDP}(4)$ utilize corresponding functions represented. The direction based structures to obtain second order LDP, has been pictorially explained in Fig. 3.2, here it is mandatory to consider that the positions of G_c and G_i are inter-changeable based on the place of corresponding pixel with respect to center pixel. Second order LDP has been calculated with the use of Eq. (8), (9), and (10).

Table 3.1: All possible local pattern combinations for four angle structures

Structures for all four angles (0^0, 45^0, 90^0, 135^0)	Pattern Combination
$S_{LDP}(1)$	$p(G_c, G_1)$, $p(G_c, G_5)$
$S_{LDP}(2)$	$p(G_c, G_2)$, $p(G_c, G_6)$
$S_{LDP}(3)$	$p(G_c, G_3)$, $p(G_c, G_7)$
$S_{LDP}(4)$	$p(G_c, G_4)$, $p(G_c, G_8)$

LDP [12] operator generates a 32-bit binary code for a corresponding pixel by considering two neighboring pixels and a comparison result has drawn based on derivative directions of these neighborhood pixels. Eq. (3) explains comparison method of derivative direction. LDP has been generated based on the change in these derivative directions. It can be seen that structure $S_{LDP}^{90}(3)$ represent computation of LDP for 90^0 angled pixels G_3 and G_7 with respect to center pixel G_c. Similarly, remaining structures define the LDP computation for their respective angles.

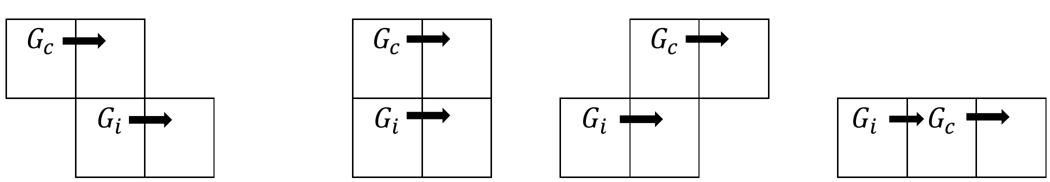

$S_{LDP}^{0}(1)$ $S_{LDP}^{0}(2)$ $S_{LDP}^{0}(3)$ $S_{LDP}^{0}(4)$

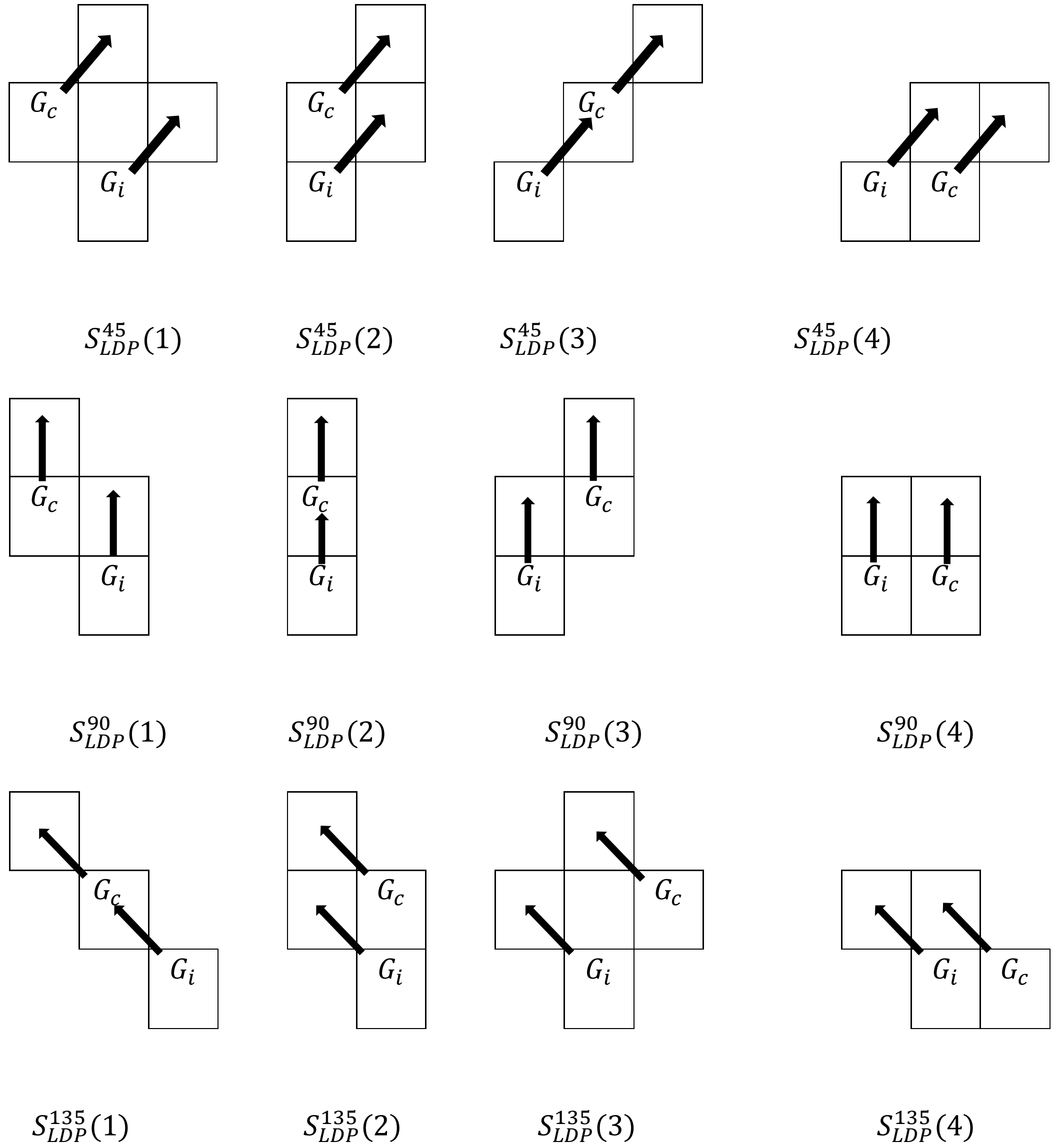

Figure 3.2. All possible structures to obtain 2nd order LDP

A 5×5 sample matrix having 3 as center pixel is shown in Fig. 3.1 (b). Considering this array as an example the computation of 2nd order LDP for 0^0 angle is pictorially explained in Fig. 3.3. The LDP encodes according to derivative direction on G_c and G_i with respect to next pixel using Eq. (3-10). Fig. 3.2 shows possible combinations of structures to get LDP in four directions.

2	1	5	6	4
3	**7**	2	1	9
5	5	**3**	7	6
6	4	5	4	3
1	3	9	7	1

(a) bit = 1

2	1	5	6	4
3	7	**2**	1	9
5	5	**3**	7	6
6	4	5	4	3
1	3	9	7	1

(b) bit = 1

2	1	5	6	4
3	7	2	**1**	9
5	5	**3**	7	6
6	4	5	4	3
1	3	9	7	1

(c) bit = 0

2	1	5	6	4
3	7	2	1	9
5	5	**3**	**7**	6
6	4	5	4	3
1	3	9	7	1

(d) bit = 1

2	1	5	6	4
3	7	2	1	9
5	5	**3**	7	6
6	4	5	4	3
1	3	9	7	1

(e) bit = 1

2	1	5	6	4
3	7	2	1	9
5	5	**3**	7	6
6	4	**5**	4	3
1	3	9	7	1

(f) bit = 1

2	1	5	6	4
3	7	2	1	9
5	5	**3**	7	6
6	**4**	5	4	3
1	3	9	7	1

(g) bit = 0

2	1	5	6	4
3	7	2	1	9
5	**5**	**3**	7	6
6	4	5	4	3
1	3	9	7	1

(h) bit = 1

Figure 3.3. Example to obtain 2nd order LDP for zero-degree angle.

As seen from Table 3.2, the calculated 2nd order LDP in all four directions for a given sample matrix has been represented. Thus the combined 32-bit second order LDP is 11011101011111000110101111011001.

Table 3.2: Computed 2nd order LDP

Angle	Computed LDP of 2nd order $LDP^2(Gc)$
0^0	11011101
45^0	01111100
90^0	01101011
135^0	11011001

To calculate 3rd order LDP, at first 2nd order derivatives towards 0^0, 45^0, 90^0, and 135^0 has been calculated which denoted as G_θ^2 where 2 represent order of LDP and θ represent angle, then use Eq. (3-10) as shown in Eq. (11-12).

$$G_\theta^3 = p\{G_\theta^2 \; of \; neighborhood \; pixels\} \tag{11}$$

$$G_\theta^n = p\left\{ G_\theta^{n-1} \; of \; neighborhood \; pixels\right\} \tag{12}$$

Hence to obtain n^{th} order LDP as shown in Eq. (12), $(n-1)^{th}$ order derivative should be computed. The performance of higher order LDP is superior over LBP for face detection and recognition application.

3.3 Local ternary patterns (LTP)

If there is large alteration in the pose, illumination, facial expression, partial occlusion, and aging then, to find the discriminative descriptor for face recognition system is a big challenge. To locate the solution of such challenges, Tan *et al.* [13], proposed LTP, which is the generalized form of LBP. It is an efficient and straightforward preprocessing method that preserves essential information for recognition and eliminates the impact due to variations in illuminations. LTP has better discrimination ability and less sensitivity to noise over LBP.

LBP has larger sensitivity to random noise where some of the regions like forehead and cheeks have been quantized in an image of the face. It is the biggest limitation of LBP in facial recognition system therefore to overcome it the extended version of LBP i.e. LTP has proposed [13], which has used 3-level quantization to get the binary pattern. LTP has better computational efficiency and higher resistance to noise.

LTP is three-valued code which is calculated using threshold range of ±T around center pixel gray value G_c (G_c ± T). If the difference between neighbor pixel gray value and center pixel gray value falls within this range, it is quantized to 0, difference above this range is quantized to +1, and difference below this range is quantized to -1 as shown below in Eq. (13).

$$G_{LTP}(Gi, Gc, T) = \begin{cases} +1, & if\ Gi\ \geq (Gc+T); \\ 0, & if\ |Gi-Gc| < T; \\ -1, & if\ Gi\ \leq (Gc-T); \end{cases} \quad Where\ T\ is\ threshold; \tag{13}$$

10	9	4
11	**6**	16
2	7	3

(a)

An example 3×3 matrix

1	1	0
1		1
0	1	0

(b)

Computed LBP = 11010101

10	9	5
11	6±2	16
2	7	3

(b)

Considering ±2 Threshold,

[4,8] Threshold range

1	1	0
1		1
-1	0	-1

(d)

computed LTP = 1101(-1)0(-1)

1	1	0
1		1
0	0	0

(e)

Upper LTP

Binary Code = 11010001

0	0	0
0		0
1	0	1

(f)

Lower LTP

Binary code = 00001010

Figure 3.4. An illustration of Local ternary pattern computation

Eq. (13) describes the concept of computation of LTP. Fig. 3.4 explains formulation of LTP with an example of the 3×3 matrix as shown in Fig. 3.4 (a). In this example, LBP for a center pixel gray value 6, has computed using Eq. (1), as shown in Fig.3.4 (b). Using the Eq. (10) in the example shown in Fig.3.4 (a), considering ±2 as threshold (4 to 8 as quantization range) the calculated LTP is 1101(-1)0(-1) as shown in Fig. 3.4 (d). The three valued function $G_{LTP}(Gi, Gc, T)$ further converted to two separate binary codes, one for +1 value is 1101000 as shown in Fig. 3.4 (e) which is called Upper LTP and another for -1 value is 00001010 as depicted in Fig. 3.4 (f) which is called Lower LTP.

LTP is an extended form of LBP which is a robust descriptor in varying lighting conditions. It has proposed preprocessing algorithm whose identification performance is better than the existing normalization of illumination theory. The performance of LTP in noise constraints is better than the LBP.

3.4 Local tetra patterns (LTrP)

Murala *et. al* [14], implemented the theory of local tetra patterns. Given an image A, consider a sample 3×3 gray value pixel matrix shown in Figure 1.1(a). Let $D_{\emptyset}(Gi)$ denote the 1st order derivative of pixel G_i, where $\emptyset$ is angle towards G_i from center pixel G_C. Let G_V and G_H represent vertical and horizontal neighborhood of center pixel G_C , so function $D_{\emptyset}(Gc)$ for angles 0° and 90° is given as shown in below Eq. (14) and (15),

$$D_{0^\circ}(Gc) = A(G_H) - A(G_C); \tag{14}$$

$$D_{90^\circ}(Gc) = A(G_V) - A(G_C); \tag{15}$$

$$D_{Dir.}(G_C) = \begin{cases} 1, & if\ D_{0^\circ}(Gc) \geq 0\ and\ D_{90^\circ}(Gc)\ \geq 0\,; \\ 2, & if\ D_{0^\circ}(Gc) < 0\ and\ D_{90^\circ}(Gc)\ \geq 0\,; \\ 3, & if\ D_{0^\circ}(Gc) < 0\ and\ D_{90^\circ}(Gc)\ < 0\,; \\ 4, & if\ D_{0^\circ}(Gc) \geq 0\ and\ D_{90^\circ}(Gc)\ < 0\,; \end{cases} \tag{16}$$

The center pixel directional calculation is done through Eq. (16). It can be seen from this equation the possible four directional tetra code i.e. 1, 2, 3, and 4 has been computed for a center pixel which is utilized to generate the LTrP that further explained by a detail pictorial representation shown in Fig. 3.5. The second order LTrP^2 (G_C) is given as

$$LTrP^2(G_C) = \begin{Bmatrix} F\big(D_{Dir.}(G_C), D_{Dir.}(G_1)\big), F\big(D_{Dir.}(G_C), D_{Dir.}(G_2)\big), \dots \\ \dots\dots\dots\dots\dots\dots\dots\dots\dots\dots\dots\dots . F\big(D_{Dir.}(G_C), D_{Dir.}(G_8)\big) \end{Bmatrix} \quad (17)$$

$$F\big(D_{Dir.}(G_C), D_{Dir.}(G_i)\big) = \begin{cases} 0, & if\ D_{Dir.}(G_C) = D_{Dir.}(G_i); \\ D_{Dir.}(G_i), & else; \end{cases} \quad (18)$$

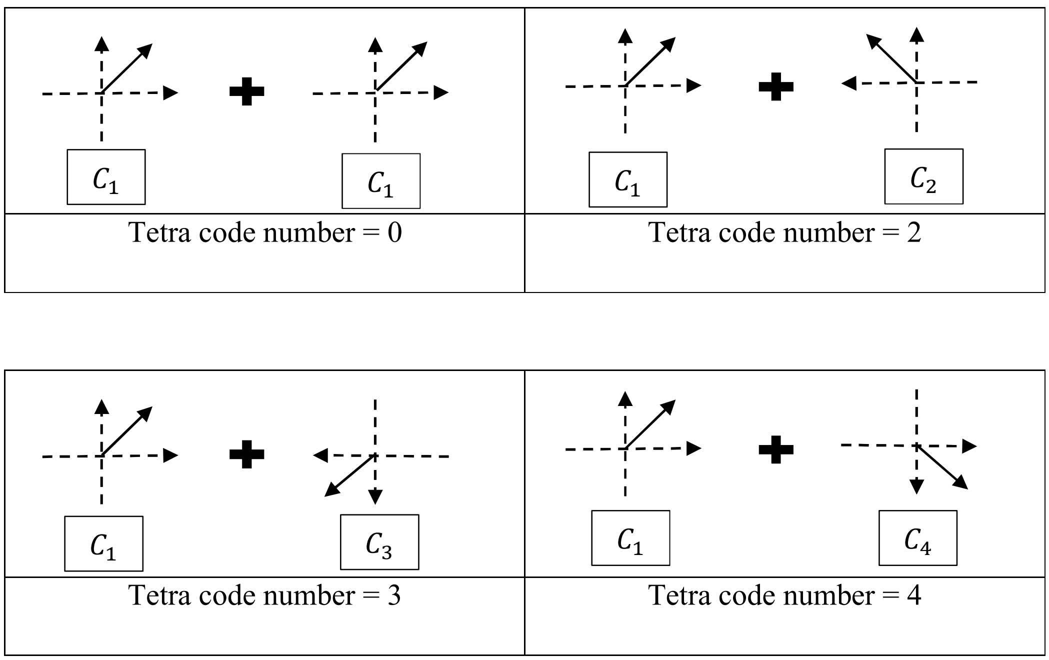

Figure 3.5. Combinations of directional templates for Tetra pattern formation

The Fig. 3.5 shows directional combinations for assigning tetra value to the particular pixel template on center pixel template. According to horizontal and vertical neighbor pixel direction, the four coordinates have depicted as C_1, C_2, C_3, and C_4. The possible tetra code values are assigned based on combinations of center pixel coordinate template and considered pixel coordinate template.

A simple example of computation of LTrP is illustrated in the Fig. 3.6. Let a 5×5 example pixel value matrix of an image as shown in Fig. 3.6 (a).

7	1	5	8	1
9	6	7	6	4
5	1	**3**	8	7
7	4	9	5	6
6	2	8	3	9

(a) Center pixel 3 in Coordinate C_1

7	1	5	8	1
9	**6**	7	6	4
5	1	**3**	8	7
7	4	9	5	6
6	2	8	3	9

(b) Pixel value 6 in Coordinate C_4

$(C_1 + C_4)$ Tetra code = 4

7	1	5	8	1
9	6	**7**	6	4
5	1	**3**	8	7
7	4	9	5	6
6	2	8	3	9

(c) Pixel value 7 in Coordinate C_3

$(C_1 + C_3)$ Tetra code = 3

7	1	5	8	1
9	6	7	**6**	4
5	1	**3**	8	7
7	4	9	5	6
6	2	8	3	9

(d) Pixel value 6 in Coordinate C_2

$(C_1 + C_2)$ Tetra code = 2

7	1	5	8	1
9	6	7	6	4
5	1	**3**	**8**	7
7	4	9	5	6
6	2	8	3	9

(e) Pixel value 8 in Coordinate C_3

$(C_1 + C_3)$ Tetra code = 3

7	1	5	8	1
9	6	7	6	4
5	1	**3**	8	7
7	4	9	**5**	6
6	2	8	3	9

(f) Pixel value 5 in Coordinate C_1

$(C_1 + C_1)$ Tetra code = 0

7	1	5	8	1
9	6	7	6	4
5	1	**3**	8	7
7	4	**9**	5	6
6	2	8	3	9

(g) Pixel value 9 in Coordinate C_3

$(C_1 + C_3)$ Tetra code = 3

7	1	5	8	1
9	6	7	6	4
5	1	**3**	8	7
7	**4**	9	5	6
6	2	8	3	9

(h) Pixel value 4 in Coordinate C_4

$(C_1 + C_4)$ Tetra code = 4

7	1	5	8	1
9	6	7	6	4
5	**1**	**3**	8	7
7	4	9	5	6
6	2	8	3	9

(i) Pixel value 1 in Coordinate C_1

$(C_1 + C_1)$ Tetra code = 0

Figure 3.6. An illustration of generation of LTrP

The tetra value should be assigned to each of the neighborhood pixel based on stated method as depicted in Fig.3.6 (b-i).

The calculated tetra pattern for given example matrix in Fig. 3.6 (a) is shown in Table 3.3, and this tetra pattern has been converted to three binary patterns for each tetra bit except 1. The second order LTrP calculated using Eq. (17-18). The n^{th} order LTrP can be obtained by considering the $(n-1)^{th}$ derivative of concern pixel using Eq. (17-18). The upper order LTrPs are able to extract more information than to lower order LTrPs.

Table 3.3: Calculated local tetra patterns for given example in Fig. 3.6 (a)

Patterns	**Codes**
Tetra Pattern	43230340
Binary Pattern1	00100000
Binary Pattern2	01010100
Binary Pattern2	10000010

The probability of sensitivity to noise is slightly higher as the order of derivative increases. It has been observed that the performance of second order LTrP is efficient as compared to higher order LTrPs. In comparison with standard LBP and LTP, LTrP outperformed in retrieval parameters measures. Together with Gabor transform, LTrP has increased the effectiveness of descriptor performance. By computing gray value differences, the relationship between concerned pixel and its neighborhood pixels encoded in LBP and LTP while, LTrP encodes this relationship based on first order directional derivative among horizontal and vertical directions, further a generalized n^{th} order LTrP can be encoded using $(n-1)^{th}$ order directional derivative towards vertical and horizontal directions of concerned pixel and center pixel. The LTrP performance for CBIR was better than previous descriptors as described [14].

Chapter 4

Proposed descriptor: Higher-Abstraction LBP (HA-LBP)

4.1 Overview

In this chapter, a detailed description of proposed HA-LBP methodology has been discussed. HA-LBP generation algorithm has been explained in section 4.2. The types of HA-LBP according to level of neighboring pixels have been defined in sections 4.2.1 and 4.2.2. The techniques of redundancy removal and feature length reduction have been elaborated in section 4.3 and 4.4 respectively.

4.2 Generation of Higher-Abstraction LBP

The system of CBIR has many of the existing descriptors with efficient performance. Some local pattern methodologies have been discussed in detail in Chapter 3 of this thesis. In the past published works the patterns like LBP, LDP, LTP, LTrP, LTrDP, and histogram refinement algorithm mostly rely on extraction of information from nearby pixels for a considered center pixel. The performance of any descriptor in CBIR system is considered as more efficient if the descriptor is capable enough to hold most of the information contained in surrounding pixels. HA-LBP considers surrounding multiple local descriptors to attain higher abstraction of relevant information of neighborhood pixels. It is the general case of LBP which incorporate nearby multiple descriptors instead of a single descriptor used in LBP. The impact of utilizing more than one descriptor has maximized the performance of image retrieval.

As shown in Fig. 4.1 (a), we have considered a given center pixel G_C, thus there exist eight nearby radius-1 neighbors namely G_1, G_2, G_3, G_4, G_5, G_6, G_7, and G_8. Similarly, 16 nearby radius-2 neighbors G_9 to G_{24}.

G_9	G_{10}	G_{11}	G_{12}	G_{13}
G_{24}	G_1	G_2	G_3	G_{14}
G_{23}	G_8	$\boldsymbol{G_C}$	G_4	G_{15}
G_{22}	G_7	G_6	G_5	G_{16}
G_{21}	G_{20}	G_{19}	G_{18}	G_{17}

(a) 5×5 multiple LBP template

G_1	G_2	G_3
G_8	$\boldsymbol{G_C}$	G_4
G_7	G_6	G_5

(b) 3×3 LBP template

Figure 4.1. Templates for HA-LBP generation

4.2.1 Level-1 HA-LBP (L1-HALBP)

In terms of neighbors incorporated with the center pixel to form HA-LBP, there are level-1 and level-2 HA-LBP. G_{ci} is defined as the level-1 pattern where only one nearby local descriptor is assigned with center pixel G_C to form HA-LBP as shown in Fig. 4.2, where $i \in [1, 8]$.

7	1	5	8	1
9	**6**	7	6	4
5	1	**3**	8	7
7	4	9	5	6
6	2	8	3	9

(a) Center pixels G_C = 3 and G_1 = 6

L1-HALBP $\boldsymbol{G_{C1}}$

7	1	5	8	1
9	6	**7**	6	4
5	1	**3**	8	7
7	4	9	5	6
6	2	8	3	9

(b) Center pixels G_C =3 and G_2 = 7

L1-HALBP $\boldsymbol{G_{C2}}$

7	1	5	8	1
9	6	7	**6**	4
5	1	**3**	8	7
7	4	9	5	6
6	2	8	3	9

(c) Center pixels G_C = 3 and G_3 = 6

L1-HALBP G_{C3}

7	1	5	8	1
9	6	7	6	4
5	1	**3**	**8**	7
7	4	9	5	6
6	2	8	3	9

(d) Center pixels G_C = 3 and G_4 =8

L1-HALBP G_{C4}

7	1	5	8	1
9	6	7	6	4
5	1	**3**	8	7
7	4	9	**5**	6
6	2	8	3	9

(e) Center pixels G_C = 3 and G_5 = 5

L1-HALBP G_{C5}

7	1	5	8	1
9	6	7	6	4
5	1	**3**	8	7
7	4	**9**	5	6
6	2	8	3	9

(f) Center pixels G_C = 3 and G_6 = 9

L1-HALBP G_{C6}

7	1	5	8	1
9	6	7	6	4
5	1	**3**	8	7
7	**4**	9	5	6
6	2	8	3	9

(g) Center pixels G_C = 3 and G_7 = 4

L1-HALBP G_{C7}

7	1	5	8	1
9	6	7	6	4
5	**1**	**3**	8	7
7	4	9	5	6
6	2	8	3	9

(h) Center pixels G_C = 3 and G_8 = 1

L1-HALBP G_{C8}

Figure 4.2. Level-1 HA-LBP generation methodology

In Fig. 4.2 (a), the nearby neighbor G_1 has been incorporated with G_c to form level-1 HA-LBP G_{C1}, in similar manner remaining level-1 neighbors G_1 to G_8 incorporated with center pixel G_C to form level-1 HA-LBP. HA-LBP inherit the properties of surrounding neighborhood, which is higher enough to perform better retrieval rate for images in CBIR system.

4.2.2 Level-2 HALBP (L-2 HALBP)

To generate level-2 HALBP, two nearby texture descriptors have been considered with the center pixel feature descriptor.

7	1	5	8	1
9	**6**	**7**	6	4
5	1	**3**	8	7
7	4	9	5	6
6	2	8	3	9

(a) G_C = 3, G_1 = 6, and G_2 = 7

L2-HALBP G_{C12} or G_{C21}

7	1	5	8	1
9	6	**7**	**6**	4
5	1	**3**	8	7
7	4	9	5	6
6	2	8	3	9

(b) G_C = 3, G_2 = 7, and G_3 = 6

L2-HALBP G_{C23} or G_{C32}

7	1	5	8	1
9	6	7	6	4
5	1	**3**	**8**	7
7	4	9	**5**	6
6	2	8	3	9

(c) G_C = 3, G_4 = 8, and G_5 = 5

L2-HALBP G_{C45} or G_{C54}

7	1	5	8	1
9	6	7	**6**	4
5	1	**3**	**8**	7
7	4	9	5	6
6	2	8	3	9

(d) G_C = 3, G_3 = 6, and G_4 = 8

L2-HALBP G_{C34} or G_{C43}

7	1	5	8	1
9	6	7	6	4
5	1	**3**	8	7
7	4	**9**	**5**	6
6	2	8	3	9

(e) G_C = 3, G_5 = 5, and G_7 = 9

L2-HALBP G_{C56} or G_{C65}

7	1	5	8	1
9	6	7	6	4
5	1	**3**	8	7
7	**4**	**9**	5	6
6	2	8	3	9

(f) G_C = 3, G_6 = 9, and G_7 = 4

L2-HALBP G_{C67} or G_{C76}

7	1	5	8	1
9	6	7	6	4
5	**1**	**3**	8	7
7	**4**	9	5	6
6	2	8	3	9

(g) G_C = 3, G_7 = 4, and G_8 = 1

L2-HALBP G_{C78} or G_{C87}

7	1	5	8	1
9	**6**	7	6	4
5	**1**	**3**	8	7
7	4	9	5	6
6	2	8	3	9

(h) Gc = 3, G_8 = 1, and G_1 = 6

L2-HALBP G_{C81} or G_{C18}

Figure 4.3. L2-HALBP implementation methodology

The possible combinations of L2-HALBP are G_{Cij} or G_{Cji}, where $i \neq j$, $i \in [1,8]$ and $j \in [1,8]$, the pixel G_i and G_j integrated with G_c as center pixels. If $i = j$ so L2-HALBP is same as L1-HALBP. An explanation of the formation of level-2 HA-LBP is given in Fig. 4.3.

In level-2 HA-LBP, it is noticeable that $\boldsymbol{G_{Cij} = G_{Cji}}$ as can be seen in Fig.4.3 (a-h), the possible combinations have been shown to explain the concept of proposed level-2 HA-LBP. However, there are more possible combinations for L2-HALBP like $\boldsymbol{G_{C48}}$, $\boldsymbol{G_{C15}}$.

In the given explanation of the generation of HA-LBP, it is mandatory to utilize center pixels as the threshold and consider all the neighbor except center pixel for computation of the HA-LBP.

4.3 Redundancy removal

To obtain feature for a given center pixel of sample 5x5 template, considering multiple nearby local texture descriptors tend to increase the redundancy of the bits. The inclusion of redundant information will not improve the system precision and recall rate. It has been observed in HA-LBP, there is high redundancy because of the combination of multiple descriptors, which contains same gray value repeatedly. It can be removed by considering a subset of these patterns.

To reduce the redundant information, we have divided all possible local patterns into four categories based on the angle between the neighboring pixels as drawn from center pixel. We also present the precision and recall rate when all patterns (including the redundant ones) have been included.

Table 4.1: Possible combinations for classes of HA-LBP

Name of Classes	Angle between the neighborhood as drawn from the center (degree)	All possible combinations for Fig. 4.1(a)
Class-45	45	(G_1, G_2), (G_2, G_3), (G_3, G_4), (G_4, G_5), (G_5, G_6), (G_6, G_7), (G_7, G_8), (G_8, G_1).
Class-90	90	(G_1, G_3), (G_1, G_7), (G_2, G_8), (G_2, G_4), (G_5, G_7), (G_5, G_3), (G_8, G_6), (G_4, G_6).
Class-135	135	(G_1, G_4), (G_1, G_6), (G_2, G_7), (G_2, G_5), (G_3, G_8), (G_3, G_6), (G_8, G_5), (G_4, G_7).
Class-180	180	(G_2, G_6), (G_8, G_4), (G_1, G_5), (G_7, G_3).

For the matrix shown in Fig. 4.1 (a), an explanation of patterns allocation to the four classes has been given in Table 4.1.

Initially, the experiments were performed on two data-sets i.e. Brodatz [43] and Corel [42] to verify the efficiency of proposed HA-LBP for CBIR systems; the primary reason being the memory constraint because of large feature length. Further the proposed method evaluated for GHIM 10K [44] database. All these operations are performed with reduced feature-length which results in reduced number of bins in the final histogram.

4.4 Feature length reduction

In this proposed algorithm we have used a kind of uniform pattern which we refer to as reduced uniform patterns with the regular uniform patterns to improve the CBIR system performance. In the same manner, we have also found that uniform and reduced uniform patterns with more than 2 pixels in the periphery further improves the recall rate and cut down the feature length drastically.

As discussed in chapter 2.2, uniform patterns allow maximum 2 state transitions of bits if pixels in the periphery are represented in circular form. Reduced uniform patterns allow maximum 2 discontinuities when pixels expressed in circular form, but here the periphery is the minimum bounding rectangle which encloses all ones. The same is depicted in Fig. 4.4. There is length constraint on uniform and reduced uniform patterns.

Let Z is number of zeros and O represents the number of ones in the periphery then the length constraint on uniform and reduced uniform patterns are defined as $\min(O, Z) > n$. In this thesis work, n is set to 2 for all experiments. The intuition behind the operation is to capture only the intricate patterns.

As we can see from Fig.4.4 (c), reduce uniform periphery has 10 bits and uniform periphery has 12 bits in Fig. 4.4 (b).

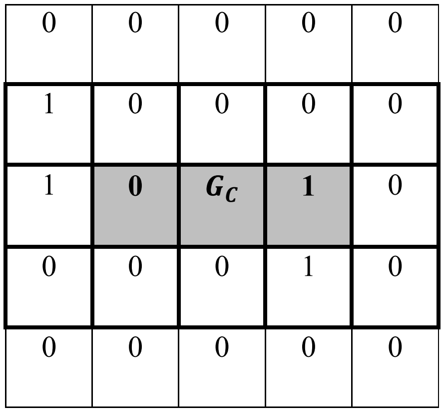

(a) G_{C48} or G_{C84}

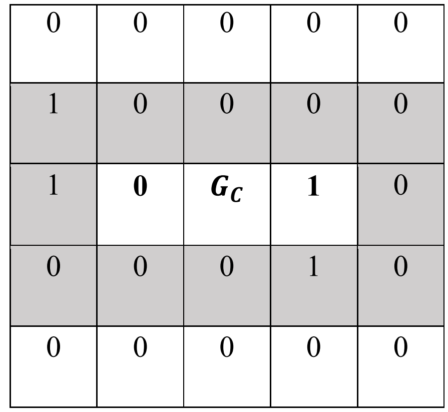

(b) Uniform Periphery

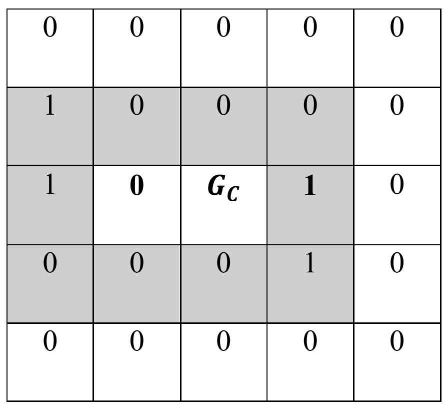

(c) Reduced Uniform periphery

Figure 4.4. Feature Length reduction by reduced uniform periphery

Chapter 5

Experimental results and discussion

5.1 Overview

In this chapter, a detailed analysis of the experiments performed using HA-LBP and a brief explanation of databases used and performance evaluation and comparison with existing methods of CBIR system based on benchmark databases has been portrayed.

5.2 Databases used and performance measures

The performance validation of proposed HA-LBP is done through experimental study on three publically available databases, *i.e.* COREL-1K database [42], BRODATZ database [43], and GHIM-10K [44] database which we named as database-1, database-2, and database-3 respectively.

To analyze performance of image retrieval, two parameters viz. precision rate and recall rate have employed.

$$Precision\ Rate = \frac{Number\ of\ images\ retrieved}{Total\ Number\ of\ images\ retrieved} \times 100\% \qquad (19)$$

$$Recall\ Rate = \frac{Number\ of\ relevant\ images\ retrieved}{Total\ Number\ of\ relevant\ images\ retrieved} \times 100\% \qquad (20)$$

The precision rate reflects the measure that out of the total images retrieved how many percentages of images are the correct set as shown in Eq. (19), and recall rate specified the precision rate of relevant images retrieved, i.e. it shows out of total relevant images retrieved how many percentages of them belongs to correct relevant retrieved images as defined in Eq. (20). The dissimilarity measurement of histogram features of query image and database images has been computed by relative l_1 metric [25].

5.3 Results on database-1

To test the performance of HA-LBP, we first performed an experiment on database-1. This database has images of size 256×384 or 384×256 and contains nature scenes, animals and games. It has 10 categories having 100 images per category.

Table 5.1: Comparison of performance of HA-LBP with existing descriptors on COREL-1000 database

Texture Descriptors	Precision rate (%)	Recall rate (%)
LBP	68.99	44.28
LDP	69.72	43.40
LTP	69.28	41.95
LTrP	67.61	46.98
LGBP	71.60	46.49
LTriDP	63.80	40.25
NRLBP	67.08	40.80
RLTP	68.30	44.30
LBP-HF	61.60	37.81
HA-LBP Class-45	**73.83**	**47.478**
HA-LBP Class-90	**73.86**	**47.406**
HA-LBP Class-135	**74.62**	**47.912**
HA-LBP Class-180	**74.13**	**48.314**
HA-LBP	**74.59**	**47.93**

The precision rate (Eq. 19) and recall rate (Eq. 20) is the commonly used performance measure which we employed in this experiment.

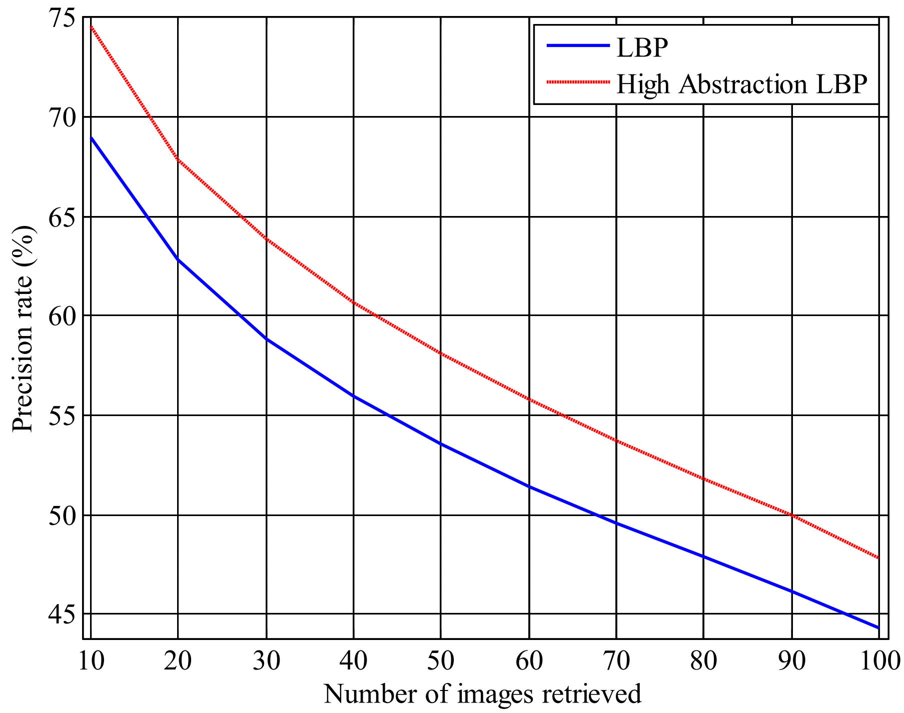

Figure 5.1. Performance evaluation curve for precision rate (%) of LBP and HA-LBP on COREL-1K database with respect to number of images retrieved.

As we see from the given Table 5.1, the retrieval performance of introduced HA-LBP as precision rate the improvement is 5.6%, 4.87%, 5.31%, 6.98%, 2.99%,10.79%, 7.51%, 6.29%, 12.99% and in terms of recall rate the improvement is 3.65%, 4.53%, 5.98%, 0.95%, 1.44%, 7.68%, 7.13%, 3.63%, 10.12%, respectively as compared with the existing descriptors LBP, LDP, LTP, LTrP, LGBP, LTriDP, NRLBP, RLTP, LBP-HF.

5.3 Results on database-2

We considered database-2 for the second experiment. It consists of 500 images of size either 300×400 pixels or 400×300 pixels for each of the category having contents such as car, insect, mountains, flower, ship, building and sunset. There are 20 such categories in this 10000 image database.

The performance of our proposed HA-LBP texture descriptor on database-2 in terms of precision rate (19) and recall rate (20) has been illustrated in Table 5.2.

Table 5.2: Performance analysis for GHIM-10000 database.

Texture descriptors	Precision rate (%)	Recall rate (%)
LBP	52.56	21.95
LDP	54.13	21.78
LTP	57.27	22.80
LTrP	54.66	21.13
LGBP	52.52	21.12
LTriDP	51.82	21.50
NRLBP	52.29	22.10
RLTP	52.80	23.37
LBP-HF	47.31	19.87
HA-LBP	**60.03**	**24.76**

For database-2, proposed HA-LBP achieved 7.47%, 5.9%, 2.75%, 5.37%, 7.51%, 8.21%, 7.74%, 7.23%, 12.72% of precision rate gain and 2.81%, 2.98%, 1.96%, 3.63%, 3.64%, 3.26%, 2.66%, 1.39%, 4.89% recall rate gain as compared to LBP, LDP, LTP, LTrP, LGBP, LTriDP, NRLBP, RLTP, LBP-HF respectively.

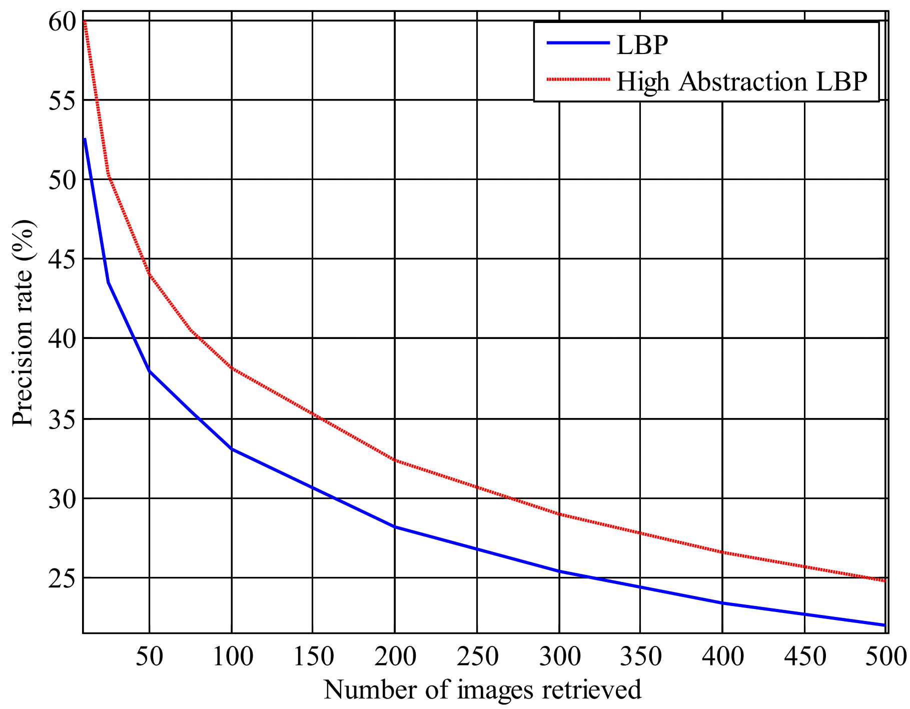

Figure 5.2 Performance evaluation curve for precision rate (%) of LBP and HA-LBP on GHIM-10K database with respect to number of images retrieved.

5.4 Results on database-3

For further performance evaluation of HA-LBP, we chose database-3. It contains 109 texture images of size 512×512, each of the image has different and unique texture, and hence there are total 109 categories of images. Each group of image has divided into 16 non-overlying sub-categories each of size 128×128. Hence there are total 1744 images in the databse-3.

The obtained result comparison of HA-LBP with existing descriptors regarding precision rate (19) and recall rate (20), is depicted in Table 5.3.

Table 5.3: Performance analysis on BRODATZ database.

Texture descriptors	Precision rate (%)	Recall rate (%)
LBP	80.23	80.23
LDP	76.15	76.15
LTP	81.12	81.12
LTrP	72.22	72.22
LGBP	78.25	78.25
LTriDP	61.80	61.80
NRLBP	80.22	80.22
RLTP	80.50	80.50
LBP-HF	80.53	80.53
HA-LBP	**82.59**	**82.59**

The precision rate and recall rate are same for brodatz texture database. As observed from Table 5.3, the proposed HA-LBP has outperformed in database-3 and opted gain over the precision as well as recall rate of existing texture descriptors viz. LBP, LDP, LTP, LTrP, LGBP, LTriDP, NRLBP, RLTP, LBP-HF of 2.36%, 6.44%, 1.47%, 10.37%, 4.34%, 20.79%, 2.37%, 2.09%, 2.06% respectively.

Chapter 6

Conclusion and scope for future work

6.1 Conclusion

In this thesis, we have proposed an effective texture descriptor for CBIR named as the Higher-Abstraction LBP. We combined nearby multiple local descriptors to obtain higher abstraction of neighborhood pixels with the use of proposed redundancy removal and feature length reduction techniques.

As seen from chapter 5, proposed HA-LBP has given excellent results in experiments performed on three databases. As compared to LBP, we observed significant improvements in performance of HA-LBP in regards with precision rate and recall rate, which are summarize below,

1) For database-1 there is 5.6% and 3.65% gain in precision rate and recall rate respectively.

2) For database-2 there is 7.47% and 2.81% increase in precision and recall rate respectively.

3) For database-3 there is 2.36% gain in precision rate as well as recall rate.

6.2 Scope for future work

In this approach, we considered nearby level-1 and level-2 local texture descriptors for the formation of HA-LBP. In future, it can be considered up to n surrounding neighbors. There can be an increase in computational complexity by considering n nearby pixels with center pixel which may lead to an enhancement in retrieval performance.

REFERENCES

[1] Y. Liu, D. Zhang, G. Lu, and W.Y. Ma, "A survey of content-based image retrieval with high-level semantics," *Pattern Recogn.*, vol.40, no. 1, pp. 262–282, Jan. 2007.

[2] D. Datta, J. Joshi, J. Li, and J.Z. Wang, "Image retrieval: ideas, influences, and trends of the new age," *ACM Comput. Surv.*, vol. 40, no. 2, pp. 1-60, Apr. 2008.

[3] T. Ojala, M. Pietikainen, and D. Harwood, "A comparative study of texture measures with classification based on feature distributions," *Pattern Recogn*., vol. 29, no. 1, pp. 51–59, Jan. 1996.

[4] T. Ojala, M. Pietikainen, and T. Maenpaa, "Multiresolution gray-scale and rotation invariant texture classification with local binary patterns," *IEEE Trans. Pattern Anal. Mach. Intell.*, vol. 24, no. 7, pp. 971–987, Jul. 2002.

[5] M. Pietikainen, T. Ojala, T. Scruggs, K. W. Bowyer, C. Jin, K. Hoffman, J. Marques, M. Jacsik, and W. Worek, "Rotational invariant texture classification using feature distributions," *Pattern Recogn.*, vol. 33, no. 1, pp. 43–52, Jan. 2000.

[6] Z. Guo, L. Zhang, and D. Zhang, "A completed modeling of local binary pattern operator for texture classification," *IEEE Trans. Image Process*., vol. 19, no. 6, pp. 1657–1663, Jun. 2010.

[7] H. Lategahn, S. Gross, T. Stehle, and T. Aach, "Texture classification by modeling joint distributions of local patterns with Gaussian mixtures," *IEEE Trans. Image Process*., vol. 19, no. 6, pp. 1548–1557, Jun. 2010.

[8] Z. Guo, L. Zhang, and D. Zhang, "Rotation invariant texture classification using LBP variance with global matching," *Pattern Recogn*., vol. 43, no. 3, pp. 706–719, Mar. 2010.

[9] S. Liao, M. W. K. Law, and A. C. S. Chung, “Dominant local binary patterns for texture classification,” *IEEE Trans. Image Process.*, vol. 18, no. 5, pp. 1107–1118, May 2009.

[10] D. Unay, A. Ekin, and R. S. Jasinschi, “*Local structure-based region-of-interest retrieval in brain MR images*,” *IEEE Trans. Inf. Technol. Biomed.*, vol. 14, no. 4, pp. 897–903, Jul. 2010.

[11] B.S. Manjunath, and W.Y. Ma, “Texture features for browsing and retrieval of image data,” *IEEE Trans. Pattern Anal. Mach. Intell.*, vol. 18, no. 8, pp. 837–842, Aug. 1996.

[12] Zhang, Y. Gao, S. Zhao, and J. Liu, “Local derivative pattern versus local binary pattern: Face recognition with higher-order local pattern descriptor,” *IEEE Trans. Image Process.*, vol. 19, no. 2, pp. 533–544, Feb. 2010.

[13] X. Tan, and B. Triggs, “Enhanced local texture feature sets for face recognition under difficult lighting conditions,” *IEEE Trans. Image Process.*, vol. 19, no. 6, pp. 1635–1650, Jun. 2010.

[14] S. Murala, R.P. Maheshwari, and R. Balasubramanian, “Local tetra patterns: a new feature descriptor for content-based image retrieval,” *IEEE Trans. Image Process.*, vol. 21, no. 5, pp. 2874–2886, Apr. 2012.

[15] K.C. Fan, and T.Y. Hung, “A novel local pattern descriptor—local vector pattern in high order derivative space for face recognition,” *IEEE Trans. Image Process.*, vol. 23, no. 7, pp. 2877–2891, Jul. 2014.

[16] W. Zhang, S. Shan, W. Gao, and H. Zhang, “Local Gabor binary pattern histogram sequence (LGBPHS): A novel non-statistical model for face representation and recognition,” in: *Proceedings of the International*

Conference on Computer Vision (ICCV), Washington DC, USA, 2005, pp. 786-791.

[17] M. Verma, and B. Raman, “Local tri-directional patterns: a new texture feature descriptor for image retrieval,” *Digit. Signal Process*., vol. 51 issue C, pp. 62–72, Apr. 2016.

[18] S. Murala, R.P. Maheshwari, and R. Balasubramanian, “Directional local extrema patterns: a new descriptor for content based image retrieval,” *Int. J. Multimed. Inf. Retr*., vol. 1, no.3, pp 191–203, Mar. 2012.

[19] S. Murala, R.P. Maheshwari, and R. Balasubramanian, “Local maximum edge binary patterns: a new descriptor for image retrieval and object tracking,” *Signal Process*., vol. 92, no. 6, pp. 1467–1479, Jun. 2012.

[20] T. Ahonen, J. Matas, C. He, and M. Pietikainen, “Rotation invariant image description with local binary pattern histogram Fourier features,” in: *Proceedings of the 16th Scandinavian Conference on Image Analysis*, Oslo, Norway, 2009, pp. 61-70.

[21] J. Ren, X. Jiang, and J. Yuan, “Noise-resistant local binary pattern with an embedded error-correction mechanism,” *IEEE Trans. Image Process.*, vol. 22, no. 10, pp. 4049–4060, Jun. 2013.

[22] J. Ren, X. Jiang, and J. Yuan, “Relaxed local ternary pattern for face recognition,” in: *Proceedings of the IEEE International Conference on Image Processing (ICIP),* Melbourne, Australia, 2013, pp. 3680–3684.

[23] A. Tiwari, V. Kanhangad, R.B. Pachori, and B.K.Panigrahi, “Automated diagnosis of epilepsy using key-point based local binary pattern of EEG signals,” *IEEE Journal of Biomedical and Health Informatics* , volume: pp, Issue: 99, 12 Jul. 2016.

[24] A. Tiwari, V. Kanhangad, and R. B. Pachori, "Histogram refinement for texture descriptor based image retrieval," *Signal processing: image communication,* vol. 53, pp. 73-85, Apr. 2017.

[25] V. Takala, T. Ahonen, and M. Pietikainen, "Block-based methods for image retrieval using local binary patterns," in: *Proceedings of the Scandinavian Conference on Image Analysis*, Joensuu, Finland, 2005, pp. 882–891.

[26] J. Trefny, and J. Matas, "Extended set of local binary patterns for rapid object detection," in: *Proceedings of the Computer Vision Winter Workshop*, Novehrady, Czech Republic, 2010, pp. 37-43.

[27] G. Zhao, and M. Pietikinen, "Dynamic texture recognition using local binary patterns with an application to facial expressions," *IEEE Trans. Pattern Anal. Mach. Intell*., vol. 27, no. 6, pp. 915–928, Jun. 2007.

[28] D. Huang, C. Shan, M. Ardabilian, Y. Wang, and L. Chen, "Local binary patterns and its application to facial image analysis: a survey,"*IEEE Trans. Syst., Man, Cybern.C, Appl. Rev.*,vol. 41, no. 6, pp. 765–781, Nov.2011.

[29] T. Ahonen, A. Hadid, and M. Pietikainen, "Face description with local binary patterns: Applications to face recognition," *IEEE Trans. Pattern Anal. Mach. Intell.*, vol. 28, no. 12, pp. 2037–2041, Dec. 2006.

[30] X. Huang, S.Z. Li, and Y. Wang, "Shape localization based on statistical method using extended local binary pattern," in: *Proceedings of the 3rd International Conference on Image and Graphics*, Washington DC, USA, 2004, pp. 184–187.

[31] V. Bajaj and R.B. Pachori, "Epileptic Seizure Detection Based on the Instantaneous Area of Analytic Intrinsic Mode Functions of EEG Signals", *Biomedical Engineering Letters*, vol. 3, pp. 17-21, 2013.

[32] R. B. Pachori and S. Patidar, “Epileptic seizure classification in EEG signals using second-order difference plot of intrinsic mode functions,” *Computer Methods Programs in Biomedicine*, vol. 113, issue 2, pp. 494-502, Feb. 2014.

[33] F. Mormann et al., “Seizure prediction: the long and winding road,” *Brain*, vol. 130, pp. 314-333, 2007.

[34] Q. Yuan, W. Zhou, S. Li, and D. Cai, “Epileptic EEG classification based on extreme learning machine and nonlinear features,” *Epilepsy Res*. 96 (1–2) (2011) 29–38.

[35] N. Päivinen, S. Lammi, A. Pitkänen, J. Nissinen, M. Penttonen, and T. Grönfors, Epileptic seizure detection: “*a nonlinear viewpoint*,” Comput. Methods Programs Biomed. 79 (2) (2005) 151–159.

[36] N. Werghi, S. Berretti, and A. Del Bimbo, “The mesh-LBP: a framework for extracting local binary patterns from discrete manifolds,” *IEEE Trans. Image Process.*, vol. 24, no. 1, pp. 220–235, Jan. 2015.

[37] J. Ryu, S. Hong, and H.S. Yang, “Sorted consecutive local binary pattern for texture classification,” *IEEE Trans. Image Process.,* vol. 24, no. 7, pp. 2254–2265, Jul. 2015.

[38] X. Qi, R. Xiao, C. Li, Y. Qiao, J. Guo, and X. Tang, “Pairwise rotation invariant co-occurrence local binary pattern,” *IEEE Trans. Pattern Anal. Mach. Intell.*, vol. 36, no. 11, pp. 2199–2213, Nov. 2014.

[39] K. Yu, Z. Wang, L. Yue, and D. Feng, “Spatially enhanced local binary pattern,” *Electron. Lett.*, vol. 48, no. 25, pp. 1590–1591, Dec. 2012.

[40] S. Liao, M.W.K. Law, and A.C.S. Chung, “Dominant local binary patterns for texture classification,” *IEEE Trans. Image Process.*, vol. 18, no. 5, pp. 1107–1118, May 2009.

[41] C.-H. Lin, C.-W. Liu, and H.-Y. Chen, "Image retrieval and classification using adaptive local binary patterns based on texture features," *IET Image Process.*, vol. 6, no. 7, pp. 822–830, Oct. 2012.

[42] Corel image database, [Online] Available: ⟨http://wang.ist.psu.edu/docs/related⟩.

[43] P. Brodatz, *Textures: A Photographic Album for Artists and Designers, Dover Publications*, New York, 1966.

[44] G.H. Liu, J.Y. Yang, Z.Y. Li, "Content-based image retrieval using computational visual attention model," *Pattern Recogn.*, vol. 48, no.8, pp. 2554–2566, Aug. 2015.